

Making graphene visible

P. Blake and E. W. Hill, A. H. Castro Neto, K. S. Novoselov, D. Jiang, R. Yang, T. J. Booth, and A. K. Geim

Citation: *Appl. Phys. Lett.* **91**, 063124 (2007); doi: 10.1063/1.2768624

View online: <http://dx.doi.org/10.1063/1.2768624>

View Table of Contents: <http://aip.scitation.org/toc/apl/91/6>

Published by the American Institute of Physics

Articles you may be interested in

[Optical constants of graphene layers in the visible range](#)

Appl. Phys. Lett. **94**, 031901 (2009); 10.1063/1.3073717

[Visibility of graphene flakes on a dielectric substrate](#)

Appl. Phys. Lett. **91**, 063125 (2007); 10.1063/1.2768625

[Counting graphene layers on glass via optical reflection microscopy](#)

Appl. Phys. Lett. **94**, 143101 (2009); 10.1063/1.3115026

[Raman Spectrum of Graphite](#)

Appl. Phys. Lett. **53**, (2003); 10.1063/1.1674108

[The effect of chemical residues on the physical and electrical properties of chemical vapor deposited graphene transferred to SiO₂](#)

Appl. Phys. Lett. **99**, 122108 (2011); 10.1063/1.3643444

[Graphene segregated on Ni surfaces and transferred to insulators](#)

Appl. Phys. Lett. **93**, 113103 (2008); 10.1063/1.2982585



Instruments for Advanced Science

Contact Hiden Analytical for further details:

W www.HidenAnalytical.com

E info@hiden.co.uk

CLICK TO VIEW our product catalogue



Gas Analysis

- dynamic measurement of reaction gas streams
- catalysis and thermal analysis
- molecular beam studies
- dissolved species probes
- fermentation, environmental and ecological studies



Surface Science

- UHV TPD
- SIMS
- end point detection in ion beam etch
- elemental imaging - surface mapping



Plasma Diagnostics

- plasma source characterization
- etch and deposition process reaction
- kinetic studies
- analysis of neutral and radical species



Vacuum Analysis

- partial pressure measurement and control of process gases
- reactive sputter process control
- vacuum diagnostics
- vacuum coating process monitoring

Making graphene visible

P. Blake^{a)} and E. W. Hill

Department of Computer Sciences, University of Manchester, Manchester M13 9PL, United Kingdom

A. H. Castro Neto

Department of Physics, Boston University, 590 Commonwealth Avenue, Boston, Massachusetts 02215

K. S. Novoselov, D. Jiang, R. Yang, T. J. Booth, and A. K. Geim

Department of Physics and Astronomy, University of Manchester, Manchester M13 9PL, United Kingdom

(Received 1 May 2007; accepted 14 June 2007; published online 10 August 2007)

Microfabrication of graphene devices used in many experimental studies currently relies on the fact that graphene crystallites can be visualized using optical microscopy if prepared on top of Si wafers with a certain thickness of SiO₂. The authors study graphene's visibility and show that it depends strongly on both thickness of SiO₂ and light wavelength. They have found that by using monochromatic illumination, graphene can be isolated for any SiO₂ thickness, albeit 300 nm (the current standard) and, especially, ≈ 100 nm are most suitable for its visual detection. By using a Fresnel-law-based model, they quantitatively describe the experimental data. © 2007 American Institute of Physics. [DOI: 10.1063/1.2768624]

Since it was reported in 2004,¹ graphene—a one-atom-thick flat allotrope of carbon—has been attracting increasing interest.^{1–3} This interest is supported by both the realistic promise of applications and the remarkable electronic properties of this material. It exhibits high crystal quality, ballistic transport on a submicron scale (even under ambient conditions) and its charge carriers accurately mimic massless Dirac fermions.^{2–4} Graphene samples currently used in experiments are usually fabricated by micromechanical cleavage of graphite: a euphemism for slicing this strongly layered material by gently rubbing it against another surface.⁵ The ability to create graphene with such a simple procedure ensures that graphene was produced an uncountable number of times since graphite was first mined and the pencil invented in 1565.⁶

Although graphene is probably produced every time one uses a pencil, it is extremely difficult to find small graphene crystallites in the “haystack” of millions of thicker graphitic flakes which appear during the cleavage. In fact, no modern visualization technique (including atomic-force, scanning-tunneling, and electron microscopies) is capable of finding graphene because of their extremely low throughput at the required atomic resolution or the absence of clear signatures distinguishing atomic monolayers from thicker flakes. Even Raman microscopy, which recently proved itself as a powerful tool for distinguishing graphene monolayers,⁷ has not yet been automated to allow search for graphene crystallites. Until now, the only way to isolate graphene is to cleave graphite on top of an oxidized Si wafer and then carefully scan its surface in an optical microscope. Thin flakes are sufficiently transparent to add to an optical path, which changes their interference color with respect to an empty wafer.¹ For a certain thickness of SiO₂, even a single layer was found to give sufficient, albeit feeble, contrast to allow the huge image-processing power of the human brain to spot a few micron-sized graphene crystallites among copious thicker flakes scattered over a millimeter-sized area.

So far, this detection technique has been demonstrated and widely used only for a SiO₂ thickness of 300 nm (purple-to-violet in color), but a 5% change in the thickness (to 315 nm) can significantly lower the contrast.² Moreover, under nominally the same observation conditions, graphene's visibility strongly varies from one laboratory to another (e.g., see images of single-layer graphene in Refs. 1 and 4), and anecdotal evidence attributes such dramatic differences to different cameras, with the cheapest ones providing better imaging.⁸ Understanding the origin of this contrast is essential for optimizing the detection technique and extending it to different substrates, aiding experimental progress in the research area.

In this letter, we discuss the origin of this optical contrast and show that it appears due not only to an increased optical path but also to the notable opacity of graphene. By using a model based on the Fresnel law, we have investigated the dependence of the contrast on SiO₂ thickness and light wavelength λ , and our experiments show excellent agreement with the theory. This understanding has allowed us to maximize the contrast and, by using narrow-band filters, to find graphene crystallites for practically any thickness of SiO₂ and also on other thin films such as Si₃N₄ and polymethyl methacrylate (PMMA).

Figure 1 illustrates our main findings. It shows graphene viewed in a microscope [Nikon Eclipse LV100D with a 100 \times , 0.9 numerical aperture (NA) objective] under normal, white-light illumination on top of a Si wafer with the standard 300 nm thickness of SiO₂ [Fig. 1(a)]. For comparison, Fig. 1(c) shows a similar sample but on top of 200 nm SiO₂, where graphene is completely invisible. In our experience, only flakes thicker than ten layers could be found in white light on top of 200 nm SiO₂. Note that the ten-layer thickness also marks the commonly accepted transition from graphene to bulk graphite.² Top and bottom panels in Fig. 1 show the same samples but illuminated through various narrow-band filters. Both flakes are now clearly visible. For 300 nm SiO₂, the main contrast appears in green [see Fig. 1(b)], and the flake is undetectable in blue light. In

^{a)}Electronic mail: peter@graphene.org

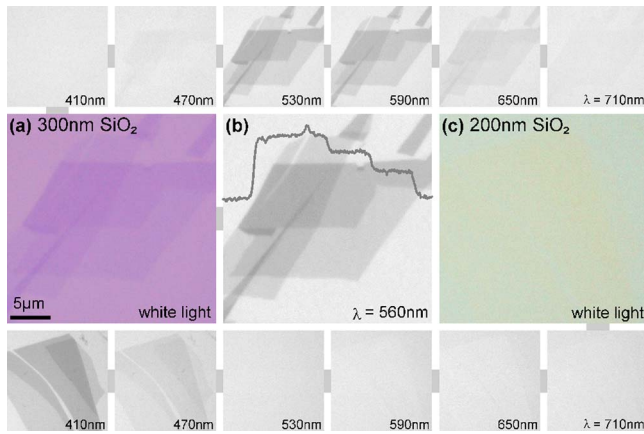


FIG. 1. (Color online) Graphene crystallites on 300 nm SiO₂ imaged with white light (a), green light and another graphene sample on 200 nm SiO₂ imaged with white light (c). Single-layer graphene is clearly visible on the left image (a), but even three layers are indiscernible on the right (c). Image sizes are 25 × 25 μm². Top and bottom panels show the same flakes as in (a) and (c), respectively, but illuminated through various narrow bandpass filters with a bandwidth of ≈ 10 nm. The flakes were chosen to contain areas of different thickness so that one can see changes in graphene's visibility with increasing numbers of layers. The trace in (b) shows steplike changes in the contrast for 1, 2, and 3 layers (trace averaged over 10 pixel lines). This proves that the contrast can also be used as a quantitative tool for defining the number of graphene layers on a given substrate.

comparison, the use of a blue filter makes graphene visible even on top of 200 nm SiO₂ (see lower panels).

To explain the observed contrast, we consider the case of normal light incidence from air (refractive index $n_0=1$) onto a trilayer structure consisting of graphene, SiO₂, and Si (see inset of Fig. 2). The Si layer is assumed to be semi-infinite

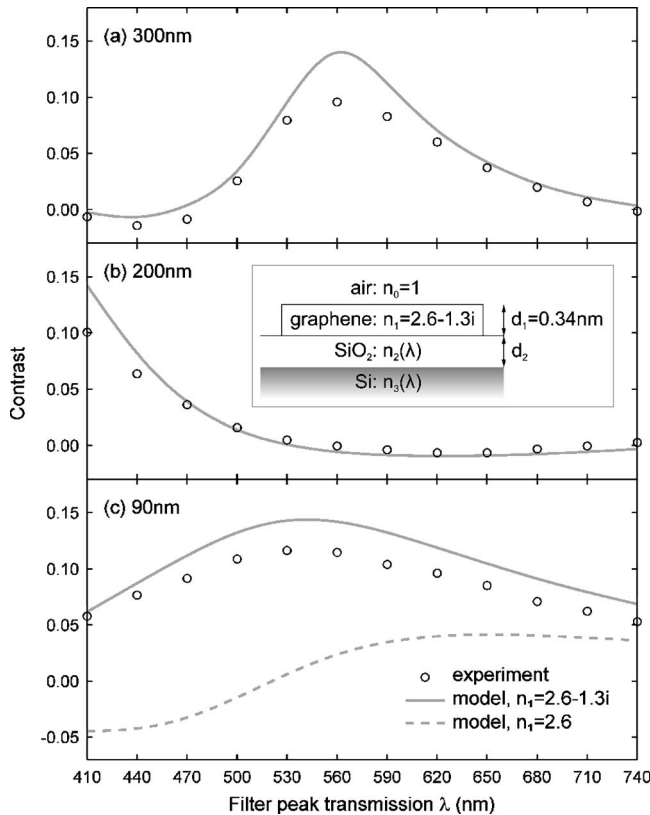


FIG. 2. Contrast as a function of wavelength for three different thicknesses of SiO₂. Circles are the experimental data; curves the calculations. Inset: the geometry used in our analysis.

and characterized by a complex refractive index $n_3(\lambda)$ that, importantly, is dependent on λ [for example, $n_3(\lambda = 400 \text{ nm}) \approx 5.6 - 0.4i$].⁹ The SiO₂ layer is described by thickness d_2 and another λ -dependent refractive index $n_2(\lambda)$ but with a real part only⁹ [$n_2(400 \text{ nm}) \approx 1.47$]. We note that these $n_2(\lambda)$ and $n_3(\lambda)$ accurately describe the whole range of interference colors for oxidized Si wafers.¹⁰ Single-layer graphene is assumed to have a thickness d_1 equal to the extension of the π orbitals out of plane¹¹ ($d_1=0.34 \text{ nm}$) and a complex refractive index $n_1(\lambda)$. While $n_1(\lambda)$ can be used in our calculations as a fitting parameter, we avoided this uncertainty after we found that our results were well described by the refractive index of bulk graphite $n_1(\lambda) \approx 2.6 - 1.3i$, which is independent of λ .^{9,12} This can be attributed to the fact that the optical response of graphite with the electric field parallel to graphene planes is dominated by the in-plane electromagnetic response.

Using the described geometry, it is straightforward to show that the reflected light intensity can be written as:¹³

$$I(n_1) = |(r_1 e^{i(\Phi_1 + \Phi_2)} + r_2 e^{-i(\Phi_1 - \Phi_2)} + r_3 e^{-i(\Phi_1 + \Phi_2)} + r_1 r_2 r_3 e^{i(\Phi_1 - \Phi_2)} \times (e^{i(\Phi_1 + \Phi_2)} + r_1 r_2 e^{-i(\Phi_1 - \Phi_2)} + r_1 r_3 e^{-i(\Phi_1 + \Phi_2)} + r_2 r_3 e^{i(\Phi_1 - \Phi_2)}) - 1|^2, \quad (1)$$

where

$$r_1 = \frac{n_0 - n_1}{n_0 + n_1},$$

$$r_2 = \frac{n_1 - n_2}{n_1 + n_2},$$

$$r_3 = \frac{n_2 - n_3}{n_2 + n_3} \quad (2)$$

are the relative indices of refraction. $\Phi_1 = 2\pi n_1 d_1 / \lambda$ and $\Phi_2 = 2\pi n_2 d_2 / \lambda$ are the phase shifts due to changes in the optical path. The contrast C is defined as the relative intensity of reflected light in the presence ($n_1 \neq 1$) and absence ($n_1 = n_0 = 1$) of graphene,

$$C = \frac{I(n_1 = 1) - I(n_1)}{I(n_1 = 1)}. \quad (3)$$

For quantitative analysis, Fig. 2 compares the contrast observed experimentally with the one calculated by using Eq. (3). The experimental data were obtained for single-layer graphene on top of SiO₂/Si wafers with three different SiO₂ thicknesses by using 12 different narrow-band filters. One can see excellent agreement between the experiment and theory. The contrast reaches up to ≈ 12%, and the peaks in graphene's visibility are accurately reproduced by our model.¹⁴ Note, however, that the theory slightly but systematically overestimates the contrast. This can be attributed to deviations from normal light incidence (because of high NA) and an extinction coefficient of graphene, $k_1 = -\text{Im}(n_1)$, that may differ from that of graphite. k_1 affects the contrast both by absorption and by changing the phase of light at the interfaces, promoting destructive interference. To emphasize the important role played by this coefficient, the dashed line in Fig. 2(c) shows the same calculations but with $k_1=0$. The

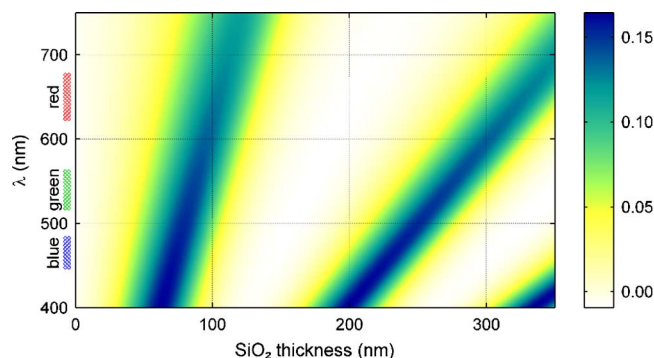


FIG. 3. (Color online) Color plot of the contrast as a function of wavelength and SiO_2 thickness according to Eq. (3). The color scale on the right shows the expected contrast.

latter curve does not bare even a qualitative similarity to the experiment, which proves the importance of opacity for the visibility of graphene.

To provide a guide for the search of graphene on top of SiO_2/Si wafers, Fig. 3 shows a color plot for the expected contrast as a function of SiO_2 thickness and wavelength. This plot can be used to select filters most appropriate for a given thickness of SiO_2 . It is clear that by using filters, graphene can be visualized on top of SiO_2 of practically any thickness, except for ≈ 150 nm and below 30 nm. Note, however, that the use of green light is most comfortable for eyes that, in our experience, become rapidly tired with the use of high-intensity red or blue illumination. This makes SiO_2 thicknesses of approximately 90 and 280 nm most appropriate with the use of green filters as well as without any filters, in white light. In fact, the lower thickness of ≈ 90 nm provides a better choice for graphene's detection (see Fig. 2), and we suggest it as a substitute for the present benchmark thickness of ≈ 300 nm.

Finally, we note that the changes in the light intensity due to graphene are relatively minor, and this allows the observed contrast to be used for measuring the number of graphene layers (theoretically, multilayer graphene can be modeled by the corresponding number of planes separated by d_1). The trace in Fig. 1(a) shows how the contrast changes with the number of layers, and the clear quantized plateaus show that we have regions of single, double, and triple layer graphene. Furthermore, by extending the same approach to other insulators, we were able to find graphene on 50 nm Si_3N_4 using blue light and on 90 nm PMMA using white light.

In summary, we have investigated the problem of visibility of graphene on top of SiO_2/Si wafers. By using the Fresnel theory, we have demonstrated that contrast can be

maximized for any SiO_2 thickness by using appropriate filters. Our work establishes a quantitative framework for detecting single and multiple layers of graphene and other two-dimensional atomic crystals⁵ on top of various substrates.

The authors thank I. Martin for illuminating discussions and C. Luke from Nikon UK for the loan of the monochrome camera.⁸ The Manchester work was supported by EPSRC (UK), and one of the authors (A.H.C.N.) by NSF under Grant No. DMR-0343790. After our letter was submitted, four preprints^{15–18} discussing the same topic appeared on the cond-mat arXiv.

¹K. S. Novoselov, A. K. Geim, S. V. Morozov, D. Jiang, Y. Zhang, S. V. Dubonos, I. V. Grigorieva, and A. A. Firsov, *Science* **306**, 666 (2004).

²A. K. Geim and K. S. Novoselov, *Nat. Mater.* **6**, 183 (2007).

³A. H. Castro Neto, F. Guinea, and N. M. R. Peres, *Phys. World* **19**, 33 (2007).

⁴Y. Zhang, J. W. Tan, H. L. Stormer, and P. Kim, *Nature (London)* **438**, 201 (2005).

⁵K. S. Novoselov, D. Jiang, F. Schedin, T. J. Booth, V. V. Khotkevich, S. V. Morozov, and A. K. Geim, *Proc. Natl. Acad. Sci. U.S.A.* **102**, 10451 (2005).

⁶H. Petroski, *The Pencil: A History of Design and Circumstance* (Knopf, New York, 1989), Chap. 4, pp. 36–47.

⁷A. C. Ferrari, J. C. Meyer, V. Scardaci, C. Casiraghi, M. Lazzeri, F. Mauri, S. Piscanec, D. Jiang, K. S. Novoselov, S. Roth, and A. K. Geim, *Phys. Rev. Lett.* **97**, 187401 (2006).

⁸Filtered light images are taken with a Nikon DS-2MBWc monochrome camera. White light images are taken with a Nikon DS-2Mv color camera. Cheaper cameras are more likely to do extensive postprocessing of images in firmware or software that could enhance contrast.

⁹*Handbook of Optical Constants of Solids*, edited by E. D. Palik (Academic, New York, 1991), 2, pp. 457–458.

¹⁰J. Henrie, S. Kellis, S. Schultz, and A. Hawkins, *Opt. Express* **12**, 1464 (2004).

¹¹Linus Pauling, *The Nature of the Chemical Bond* (Cornell University Press, Ithaca, 1960), Chap. 7, pp. 234–235.

¹²In Ref. 9, the refractive index of bulk graphite is within 5% of 2.6–1.3i between 300 and 590 nm. At 630 nm, the extinction coefficient jumps to 1.73, but this coincides with a change of reference in the handbook, which we have chosen to ignore in our model.

¹³H. Anders, *Thin Films in Optics* (Focal, London, 1967), Pt. 1, pp. 18–48.

¹⁴The experimental contrast was found by computer analysis of the images obtained using a monochrome camera Ref. 8. The thickness of SiO_2 usually differs by up to 5% from nominal values provided by suppliers and, accordingly, in our theoretical calculations in Fig. 2, the following values for d_2 were used to achieve the best fit: (a) 290 nm, (b) 190 nm, and (c) 88 nm.

¹⁵I. Jung, M. Pelton, R. Piner, D. A. Dikin, S. Stankovich, S. Watcharotone, M. Hausner, and R. S. Ruoff, e-print arXiv:cond-mat/0706.0029.

¹⁶C. Casiraghi, A. Hartschuh, E. Lidorikis, H. Qian, H. Harutyunyan, T. Gokus, K. S. Novoselov, and A. C. Ferrari, e-print arXiv:cond-mat/0705.2645.

¹⁷D. S. L. Abergel, A. Russell, and V. I. Fal'ko, e-print arXiv:cond-mat/0705.0091.

¹⁸S. Roddaro, P. Pingue, V. Piazza, V. Pellegrini, and F. Beltram, e-print arXiv:cond-mat/0705.0492.